Graph Signal Processing over Multilayer Networks – Part I: Foundations and Spectrum Analysis

Songyang Zhang, Qinwen Deng, David C. Zhu, Tongtong Li, and Zhi Ding, *Fellow, IEEE*

Abstract—Signal processing over single-layer graphs has become a mainstream tool owing to its power in revealing obscure underlying structures within data signals. For generally, many real-life datasets and systems are characterized by more complex interactions among distinct entities. Such complex interactions may represent multiple levels of interactions that are difficult to be modeled with a single layer graph and can instead be captured by multiple layers of graph connections. Such multilayer/multi-level data structure can be more naturally modeled and captured by a high-dimensional multi-layer network (MLN). This work generalizes traditional graph signal processing (GSP) over multilayer networks for analysis of such multilayer signal features and their interactions. We propose a tensor-based framework of this multilayer network signal processing (M-GSP) in this two-part series. Specially, Part I introduces the fundamentals of M-GSP and studies spectrum properties of MLN Fourier space. We further describe its connections to traditional digital signal processing and GSP. Part II focuses on several major tools within the M-GSP framework for signal processing and data analysis. We provide results to demonstrate the efficacy and benefits of applying multilayer networks and the M-GSP in practical scenarios.

Index Terms—Multilayer network, graph signal processing, tensor, data analysis

I. Introduction

GEOMETRIC signal processing models have found broad applications in data analysis to uncover obscure or hidden structures from complex datasets [1]. Various data sources, such as social networks, traffic flows, and biological images, often feature complex structures that pose challenges to traditional signal processing tools [2]. Recently, graph signal processing (GSP) emerges as an effective tool over the graph signal representation [3]. For a signal with N samples, a graph of N nodes can be formed to model their underlying interactions. In GSP, a graph Fourier space is also defined from the spectral space of the representing matrix (adjacency/Laplacian) for signal processing tasks [4], such as denoising [5], resampling [6], and classification [7]. Generalization of the more traditional GSP includes signal processing over hypergraphs [8] and simplicial complexes [9], which are suitable to model high-degree multi-lateral node relationships.

Traditional graph signal processing tools generally describe signals as graph nodes connected by one type of edges [10]. Real-life systems and datasets may feature multi-facet

S. Zhang, Q. Deng and Z. Ding are with Department of Electrical and Computer Engineering, University of California, Davis, CA, 95616. (E-mail: sydzhang@ucdavis.edu, mrdeng@ucdavis.edu, and zding@ucdavis.edu).
D. C. Zhu and T. Li are with Michigan State University, MI, 48824. (E-mail: David.Zhu@radiology.msu.edu, and tongli@egr.msu.edu.)

interactions [11]. For example, in a video dataset modeled by the spatial temporal graph shown in Fig. 1(a), the nodes could have different types of spatial connections at different temporal steps. Single-layer graphs are not equipped to model such multi-facet connections. To model multiple layers of signal connectivity, we explore a high-dimensional graph representation known as multilayer networks [12]. The multilayer network (MLN) is a geometric model containing correlated layers with different structures and physical meanings, unlike traditional single-layer graphs. MLN cannot be replaced by a single graph since different layers represent different signal characteristics. A typical example is smart grid consisting of two layers shown as Fig. 1(b): the power grid and the computation network. These two layers have different physical connectivity and rules [13]. On the other hand, signal interactions across the multiple layers in MLN can be strongly correlated. Thus, separate representations by multiple single layer graphs would fail to capture such characteristics. Consider a network consisting of a physical power layer and a cyber layer, the failure of one layer could trigger the failure of the other [14]. One example was the power line damage caused by a storm on September 28th of 2003. It not only led to the failure of several power stations, but also disrupted communications as a result of power station breakdowns that eventually affected 56 million people in Europe [15].

Our goal is to generalize graph signal processing onto multilayer networks to model, analyze, and process signals based on the *intralayer* and *interlayer* signal interactions.
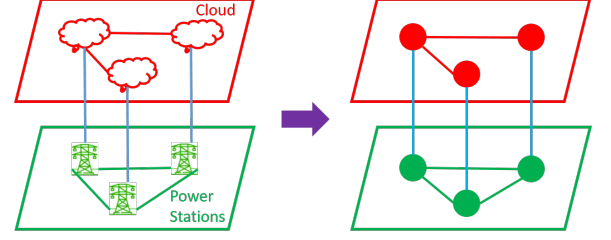
To develop a signal processing framework for MLN, one needs to process interlayer connections and intralayer connections consistently. In [16], a two-step transform is proposed to process spatial-temporal graphs. Graph Fourier transform (GFT) is applied first in the spatial domain (intralayer) and then in the temporal domain (interlayer). In this framework, different graph Fourier spaces are defined for interlayer and intralayer connections respectively. However, a spectral space to jointly capture the interlayer and intralayer information remains a problem. In [17], a joint time-vertex Fourier transform (JFT) is defined by implementing GFT and DFT consecutively. Although JFT can process the time-varying datasets, it is unable to process more general temporal (interlayer) connectivity in a generic multilayer network. Alternatively, a tensor-based multi-way graph signal processing framework (MWGSP) relies on product graph [18]. In this framework, separate factor graphs are constructed for each mode of a tensor-represented signal, and a joint spectrum is defined by combining the spectra of all factor graphs. Since MWGSP focuses on product of all factor graphs estimated from signals,
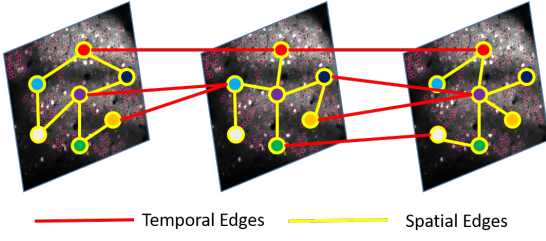
(a) Video: each layer represents one frame of the video and the edges capture the spatial-temporal relationships.

(b) Cyber-Physical System (CPS): each layer represents one component in CPS and the edges capture the physical connections.

Fig. 1. Multilayer Networks and Applications.

it is not well suited to a multilayer network with a given structure.

Another challenge in MLN signal processing is the development of a suitable mathematical representation. Traditional methods start with connectivity matrices. For example, two different matrices can represent intralayer connections and interlayer connections [19]. One can also represent each layer with an individual adjacency matrix [20]. However, such matrix-based representations exhibit certain limitations when the number of layers exceed two [19], or lack of representation for interlayer interactions [20]. A more natural and general way is to start with tensor representation [10], which is particularly attractive in handling complex MLN graph analysis.

To address the aforementioned challenges and to advance MLN signal processing, we present a novel tensor framework for graph signal processing over multilayer networks (M-GSP). We summarize the main contributions of this two-part series as follows:

- Part I focuses on the theoretical foundation of M-GSP. Leveraging tensor representation of MLN, we introduce the definitions of signals and shifting over MLN. We further define the concepts of spectral space and spectrum transform for M-GSP. For interpretability of the spectral space, we analyze the resulting MLN spectral properties and their distinctions from existing GSP tools.
- Part II [21] investigates practical tools and applications for M-GSP. We introduce alternative definitions of stationary process, convolution, and sampling over MLN for data analysis. In addition, we develop fundamentals of filter design and methods for spectrum estimation within the proposed framework. We compare the performance of MLN methods with traditional signal processing and learning algorithms in several practical applications.

In Part I of the two part series, we organize the technical contents as follows. Section II first summarizes the preliminaries of traditional GSP and tensor analysis. We then introduce the main concepts and definitions of M-GSP in Section III. We provide the physical insights and spectrum interpretation of M-GSP concepts in Section IV. Finally, we conclude the first part in Section V.

II. PRELIMINARIES

A. Overview of Graph Signal Processing

GSP is a relatively new signal processing tool defined over graphs. Here, we briefly introduce the key concepts of traditional GSP [1]–[3].

Signal processing on graphs studies signals that are discrete in some dimensions by representing the irregular signal structure using a graph $\mathcal{G} = \{\mathcal{V}, \mathbf{F}\}$, where $\mathcal{V} = \{v_1, v_2, \cdots, v_N\}$ is a set of N nodes, and $\mathbf{F} \in \mathbb{R}^N \times \mathbb{R}^N$ is the representing matrix (e.g., adjacency/Laplacian) describing the geometric structure of the graph $\mathcal{G}$. Graph signals are the attributes of nodes that underlie the graph structure. A graph signal can be written as vector

$$\mathbf{s} = [s_1, s_2, \cdots, s_N]^{\mathrm{T}} \in \mathbb{R}^N. \tag{1}$$

With a graph representation $\mathbf{F}$ and a signal vector $\mathbf{s}$, the basic graph shifting is defined via

$$\mathbf{s}' = \mathbf{F}\mathbf{s}. \tag{2}$$

The graph spectral space, also known as the graph Fourier space is defined based on the eigenspace of the representing matrix. Let the eigen-decomposition of $\mathbf{F}$ be given by

$$\mathbf{F} = \mathbf{V}\mathbf{\Sigma}\mathbf{V}^{-1}, \tag{3}$$

where $\mathbf{V}$ is the matrix with eigenvectors of $\mathbf{F}$ as columns, and diagonal matrix $\mathbf{\Sigma}$ consists of the corresponding eigenvalues. The graph Fourier transform (GFT) is defined as

$$\hat{\mathbf{s}} = \mathbf{V}^{-1}\mathbf{s}, \tag{4}$$

whereas the inverse GFT is given by

$$\mathbf{s} = \mathbf{V}\hat{\mathbf{s}}. \tag{5}$$

From definitions of GFT, other graph concepts, such as graph sampling theory [23], filter design [24], and frequency analysis [4] can be developed for signal processing and data analysis tasks.

B. Introduction of Tensor Basics

Before introducing the fundamentals of M-GSP, we first review some basics on tensors that are useful for multilayer network analysis. Tensors can be viewed as multi-dimensional arrays. The order of a tensor is the number of indices needed to label a component of that array [25]. For example, a third-order tensor has three indices. More specially, a scalar is a zeroth-order tensor; a vector is a first-order tensor; a matrix is a second-order tensor; and an M-dimensional array is an Mth-order tensor. In this two-part series, we use bold letters to represent the tensors, i.e., $\mathbf{A} \in \mathbb{R}^{I_1} \times \mathbb{R}^{I_2} \cdots \times \mathbb{R}^{I_N}$ represents an Nth-order tensor with I_k being the dimension of the kth

(a) CP Decomposition.
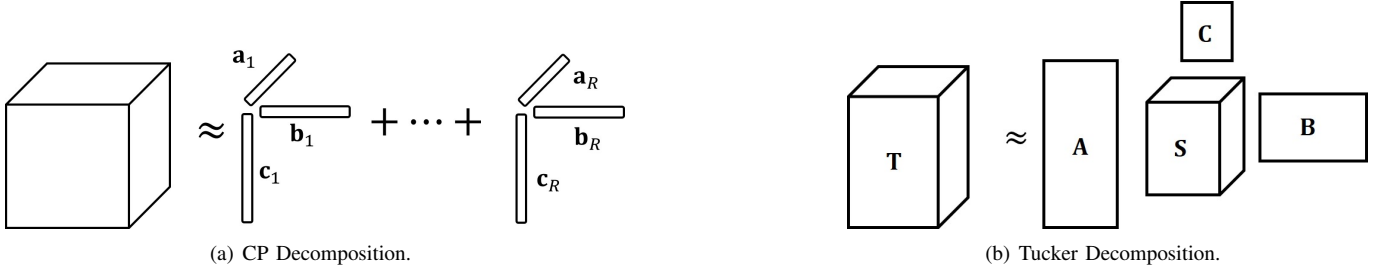

(b) Tucker Decomposition.

Fig. 2. Diagram of Tensor Decomposition.

order, and use $A_{i_1 \cdots i_N}$ to represent the entry of $\mathbf{A}$ at position $(i_1, i_2, \cdots, i_N)$ with $1 \leq i_k \leq I_k$. If $\mathbf{A}_f$ has a subscript f, we use $[A_f]_{i_1 \cdots i_N}$ to denote its entries.

We now start with some useful definitions and tenor operations for the M-GSP framework [25].

1) Super-diagonal Tensor: An Nth-order tensor $\mathbf{A} \in \mathbb{R}^{I_1} \times \mathbb{R}^{I_2} \cdots \times \mathbb{R}^{I_N}$ is *super-diagonal* if its entries $A_{i_1 i_2 \cdots i_N} \neq 0$ only for $i_1 = i_2 = \cdots = i_N$.

2) Symmetric Tensor: A tensor is *super-symmetric* if its elements remain constant under index permutation. For example, a third-order $\mathbf{A} \in \mathbb{R}^I \times \mathbb{R}^I \times \mathbb{R}^I$ is *super-symmetric* if

$$A_{ijk} = A_{jik} = A_{kij} = A_{kji} = A_{jik} = A_{jki} \quad i, j, k = 1, \cdots, I. \tag{6}$$

In addition, tensors can be *partially symmetric* in two or more modes as well. For example, a third-order tensor $\mathbf{A} \in \mathbb{R}^I \times \mathbb{R}^I \times \mathbb{R}^J$ is *symmetric* in the order one and two if

$$X_{ijk} = X_{jik}, \tag{7}$$

for $1 \leq i, j \leq I$ and $1 \leq k \leq J$.

3) Tensor Outer Product: The *tensor outer product* between an Pth-order tensor $\mathbf{U} \in \mathbb{R}^{I_1} \times \cdots \times \mathbb{R}^{I_P}$ with entries $U_{i_1 \ldots i_P}$ and an Qth-order tensor $\mathbf{V} \in \mathbb{R}^{J_1} \times \cdots \times \mathbb{R}^{J_Q}$ with entries $V_{j_1 \ldots j_Q}$ is denoted by

$$\mathbf{W} = \mathbf{U} \circ \mathbf{V}. \tag{8}$$

The result $\mathbf{W} \in \mathbb{R}^{I_1} \times \cdots \times \mathbb{R}^{I_P} \times \mathbb{R}^{J_1} \times \cdots \times \mathbb{R}^{J_Q}$ is an $(P+Q)$th-order tensor, whose entries are calculated by

$$W_{i_1 \ldots i_P j_1 \ldots j_Q} = U_{i_1 \ldots i_P} \cdot V_{j_1 \ldots j_Q}. \tag{9}$$

The tensor outer product is useful to construct a higher order tensor from several lower order tensors.

4) n-mode Product: The *n-mode product* between a tensor $\mathbf{U} \in \mathbb{R}^{I_1} \times \cdots \times \mathbb{R}^{I_P}$ and a matrix $\mathbf{V} \in \mathbb{R}^J \times \mathbb{R}^{I_n}$ is denoted by $\mathbf{W} = \mathbf{U} \times_{\mathbf{n}} \mathbf{V} \in \mathbb{R}^{I_1} \times \cdots \times \mathbb{R}^{I_{n-1}} \times \mathbb{R}^J \times \mathbb{R}^{I_{n+1}} \times \cdots \times \mathbb{R}^{I_P}$. Each element in $\mathbf{W}$ is given by

$$W_{i_1 i_2 \cdots i_{n-1} j i_{n+1} \cdots i_P} = \sum_{i_n=1}^{I_n} U_{i_1 \cdots i_P} V_{j i_n}, \tag{10}$$

where the main function is to modify the dimension of a specific order. For example, in Eq. (10), the dimension of the nth order of $\mathbf{U}$ is changed from I_n to J.

5) Hadamard Product: The *Hadamard product* between $\mathbf{U} \in \mathbb{R}^P \times \mathbb{R}^Q$ and $\mathbf{V} \in \mathbb{R}^P \times \mathbb{R}^Q$ is defined as

$$\mathbf{U} * \mathbf{V} = \begin{bmatrix} U_{11}V_{11} & U_{12}V_{12} & \cdots & U_{1Q}V_{1Q} \\ U_{21}V_{21} & U_{22}V_{22} & \cdots & U_{2Q}V_{2Q} \\ \vdots & \vdots & \ddots & \vdots \\ U_{P1}V_{P1} & U_{P2}V_{P2} & \cdots & U_{PQ}V_{PQ} \end{bmatrix}. \tag{11}$$

6) Tensor Decomposition: Tensor decompositions are useful tools to extract the underlying information of tensors. Particularly, CANDECOMP/PARAFAC (CP) decomposition decomposes a tensor as a sum of the tensor outer product of rank-one tensors [25], [26]. For example, a third order tensor $\mathbf{T} \in \mathbb{R}^I \times \mathbb{R}^J \times \mathbb{R}^K$ is decomposed by CP decomposition into

$$\mathbf{T} \approx \sum_{r=1}^{R} \mathbf{a}_r \circ \mathbf{b}_r \circ \mathbf{c}_r, \tag{12}$$

where $\mathbf{a}_r \in \mathbb{R}^I$, $\mathbf{b}_r \in \mathbb{R}^J$, $\mathbf{c}_r \in \mathbb{R}^K$ and a positive integer R is its rank, i.e., the smallest number of rank-one tensors in the decomposition. The process of CP decomposition for a third-order tensor is illustrated in Fig. 2(a), and could be interpreted as the factorization of the tensor.

Another important decomposition is the Tucker decomposition, which is in the form of higher-order PCA. More specifically, Tucker decomposition decomposes a tensor into a core tensor multiplied by a matrix along each mode [25]. Defining a core tensor $\mathbf{S} = [S_{pqr}] \in \mathbb{R}^P \times \mathbb{R}^Q \times \mathbb{R}^R$. The Tucker decomposition of a third-order tensor $\mathbf{T} \in \mathbb{R}^I \times \mathbb{R}^J \times \mathbb{R}^K$ is

$$\mathbf{T} \approx \mathbf{S} \times_1 \mathbf{A} \times_2 \mathbf{B} \times_3 \mathbf{C} \tag{13}$$

$$= \sum_{p=1}^{P} \sum_{q=1}^{Q} \sum_{r=1}^{R} S_{pqr} \mathbf{a}_p \circ \mathbf{b}_q \circ \mathbf{c}_r, \tag{14}$$

where $\mathbf{A} = [\mathbf{a}_1 \ \cdots \ \mathbf{a}_p] \in \mathbb{R}^I \times \mathbb{R}^P$, $\mathbf{B} = [\mathbf{b}_1 \ \cdots \ \mathbf{b}_Q] \in \mathbb{R}^J \times \mathbb{R}^Q$, $\mathbf{C} = [\mathbf{c}_1 \ \cdots \ \mathbf{c}_R] \in \mathbb{R}^K \times \mathbb{R}^R$ and . The diagram of the Tucker decomposition for a third-order tensor is shown in Fig. 2(b).

Note that Tucker decomposition reduces to CP decomposition if the core tensor is limited to be super-diagonal. Other typical decompositions include Higher-Order SVD (HOSVD) [27], orthogonal CP-decomposition [28], and Tensor-Train decomposition [29]. Interested readers are referred to the tutorial [25] for more details.

III. FUNDAMENTALS OF LAYERED GRAPH SIGNAL PROCESSING

In this section, we introduce the basic definitions in the proposed M-GSP framework.

(a) A three-layer interconnected network.

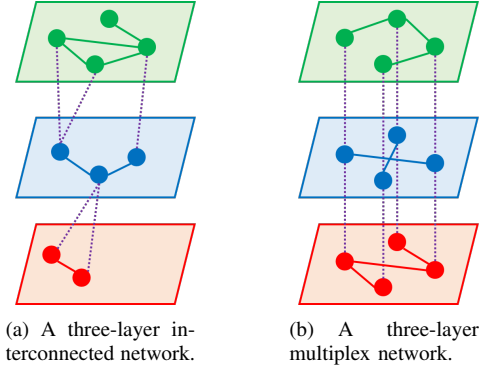(b) A three-layer multiplex network.

Fig. 3. Example of multilayer networks.

A. Multilayer Network (Layered Graph)

Before introducing the mathematical foundations of M-GSP, we first provide definitions of layered graph, also known as multilayer networks [25]. We refrain from using the "network" terminology because of its diverse meanings in various field ranging from communication networking to deep learning. From here onward, unless otherwise specified, we shall use the less ambiguous term of multi-layer graph or simply "Layered Graph" instead.

Definition 1 (Multilayer Network). *A multilayer network with K nodes and M layers is defined as* $\mathcal{M} = \{\mathcal{V}, \mathcal{L}, \mathbf{A}\}$, *where* $\mathcal{V} = \{v_1, v_2, \cdots, v_K\}$ *is the set of nodes,* $\mathcal{L} = \{l_1, l_2, \cdots, l_M\}$ *denotes the set of layers with each layer* $l_i = \{v_{i_1}, \cdots, v_{i_n}\}$ *being distinct subsets of* $\mathcal{V}$, *whereas* $\mathbf{A}$ *is the algebraic representation describing node interactions.*

In multilayer networks, edges connect nodes in the same layer (intralayer edges) or nodes in different layers (inter-layer edges) [30]. There are two main types of multilayer networks: *multiplex network* and *interconnected network* [31]. In a *multiplex network*, each layer has the same number of nodes, and each node only connects with their 1-to-1 matching counterparts in other layers to form interlayer connections. Typically, multiplex networks characterize different types of interactions among the same (or a similar) set of entities. For example, the spatial temporal connections among a set of nodes can be intuitively modeled as a multiplex network [31]. In the *interconnected networks*, each layer may have different numbers of nodes without a 1-to-1 counterpart. Their interlayer connections could be more flexible. Examples of a three-layer multiplex network and a three-layer interconnected network are shown in Fig. 3, where different colors represent different layers, the solid lines represent intralayer connections, and the dash lines indicate interlayer connections.

B. Algebraic Representation

Dynamics of multilayer networks can be captured by algebraic representation $\mathbf{A}$. To capture the high-dimensional 'multilayer' interactions between different nodes, we use tensor as algebraic representation of the multilayer networks for the proposed M-GSP framework.

To better interpret the tensor representation of a multilayer network, we start from a simpler type of multilayer networks,

in which each layer contains the same number of nodes. For a multilayer network $\mathcal{M} = \{\mathcal{V}, \mathcal{L}\}$ with $|\mathcal{L}| = M$ layers and N nodes in each layer, i.e., $|l_i| = N$ for $1 \le i \le M$, it could be interpreted as projecting the connections between a set of N entities into a set of M layers. For example, the video datasets could be modeled by the spatial connections between pixels (entities) into different temporal frames (layers). Mathematically, the process of projecting entities can be viewed as a tensor product, and network connections can be represented by tensors [10].

For convenience, we use Greek letters $\alpha, \beta, \cdots$ to indicate each layer and Latin letters $i, j, \cdots$ to indicate each interpretable "entity" with corresponding node in each layer. Given a set of entities $\mathcal{X} = \{x_1, x_2, \cdots, x_N\}$, one can construct a basis $\mathbf{e}_i \in \mathbb{R}^N$ to characterize each entity i. Thus, interactions of two entities can be represented by a second-order tensor $\mathbf{E} = \sum_{i,j=1}^{N} a_{ij} \mathbf{e}_i \circ \mathbf{e}_j \in \mathbb{R}^N \times \mathbb{R}^N$, where a_{ij} is the intensity of the relationship between entity i and j. Similarly, given a set of layers $\mathcal{L} = \{l_1, l_2, \cdots, l_M\}$, a basis $\mathbf{e}_\alpha \in \mathbb{R}^M$ can capture the properties of the layer α, and the connectivity between two layers could be represented by $\mathbf{F} = \sum_{\alpha,\beta=1}^{M} b_{\alpha\beta} \mathbf{e}_\alpha \circ \mathbf{e}_\beta \in \mathbb{R}^M \times \mathbb{R}^M$. Following this approach, connectivity between the projected nodes of the entities in the layers can be represented by a fourth-order tensor

$$\mathbf{A} = \sum_{\alpha=1}^{M} \sum_{i=1}^{N} \sum_{\beta=1}^{M} \sum_{j=1}^{N} w_{\alpha i \beta j} \mathbf{e}_\alpha \circ \mathbf{e}_i \circ \mathbf{e}_\beta \circ \mathbf{e}_j \in \mathbb{R}^M \times \mathbb{R}^N \times \mathbb{R}^M \times \mathbb{R}^N,$$
(15)

where $w_{\alpha i \beta j}$ is the weight of connection between the entity i's projected node in layer α and the entity j's projected node in layer β. More specially, if we select the basis $\mathbf{e}_i = [0, \cdots, 0, 1, 0, \cdots, 0]^\mathrm{T}$ in which the only nonzero element is the unit ith element for both layers and entities, the fourth-order tensor becomes the adjacency tensor of the multilayer network, where each entry $A_{\alpha i \beta j} = w_{\alpha i \beta j}$ characterizes the edge between the entity i's projected node in layer α and the entity j's projected node in layer β. Thus, similar to the adjacency matrix whose 2-D entries indicate whether and how two nodes are pairwise connected by a simple edge in the normal graphs, we adopt an adjacency tensor $\mathbf{A} \in \mathbb{R}^M \times \mathbb{R}^N \times \mathbb{R}^M \times \mathbb{R}^N$ to represent the multilayer network with the same number of nodes in each layer as follows.

Definition 2 (Adjacency Tensor). *A multilayer network* $\mathcal{M}$, *with* $|\mathcal{L}| = M$ *layers and* $|l_i| = N$ *nodes in each layer* i, *can be represented by a fourth-order adjacency tensor* $\mathbf{A} \in \mathbb{R}^M \times \mathbb{R}^N \times \mathbb{R}^M \times \mathbb{R}^N$ *defined as*

$$\mathbf{A} = (A_{\alpha i \beta j}), \quad 1 \le \alpha, \beta \le M, 1 \le i, j \le N. \quad (16)$$

Here, each entry $A_{\alpha i \beta j}$ *of the adjacency tensor* $\mathbf{A}$ *indicates the intensity of the edge between the entity* j's *projected node in layer* β *and entity* i's *projected node in layer* α.

Clearly, for a single layer graph/network, $\mathbf{e}_\alpha$ is a scalar 1 and the fourth-order tensor degrades to the adjacency matrix of the normal graphs. Similar to A_{ij} in an adjacency matrix which indicates the direction from the node v_j to v_i, $A_{\alpha i \beta j}$ also indicates the direction from the node $v_{\beta j}$ to the node $v_{\alpha i}$

in a layered graph/network. Note that, basis vectors $\mathbf{e}_i$ and $\mathbf{e}_\alpha$ are not spectra or eigenvectors of the adjacency tensor. They are merely the vectors characterizing connection features of the entities and layers, respectively. For the spectral space of the multilayer network based on the adjacency tensor, we shall discuss in Section III-E.

For a general multilayer network with different number of nodes in each layer, we can augment it into an equivalent multilayer reconstruction with the same number of nodes in each layer. There are mainly two ways to reconstruct: 1) Add isolated nodes to layers with fewer nodes to reach N nodes [13]; and 2) Aggregate several nodes into super-nodes for layers with $|l_i| > N$ [33]. Since isolated nodes do not interact with any other nodes, the augmentation method does not change the topological structure of the original multilayer architecture. The aggregation method, however, depends on how efficiently we can aggregate redundant or similar nodes, because this process may be lossy. For simplicity (not computation complexity), we prefer the augmentation method.

In addition, although the fourth-order adjacency tensor can be viewed as the projection of several entities into different layers in Eq. (15), the entities and layers can be virtual and not necessarily physical to capture the underlying structures of the datasets. The information within the multilayer networks, together with definitions of the underlying virtual entities and layers, should only depend on the structure of the multilayer networks. We will illustrate this further in Section IV-B.

Given an adjacency tensor, we can define the Laplacian tensor of the multilayer networks similar to that in a single layer graph. Denoting the degree (or multi-strength) of the entity's i's projected node $v_{\alpha i}$ in layer α as $d(v_{\alpha i})$, the degree tensor $\mathbf{D} \in \mathbb{R}^M \times \mathbb{R}^N \times \mathbb{R}^M \times \mathbb{R}^N$ is defined as a diagonal tensor with entries $D_{\alpha i \alpha i} = d(v_{\alpha i})$ for $1 \leq i \leq N, 1 \leq \alpha \leq M$, whereas its other entries are zero. The Laplacian tensor can be defined as follows.

Definition 3 (Laplacian Tensor). *A multilayer network $\mathcal{M}$, with $|\mathcal{L}| = M$ layers and $|l_i| = N$ nodes in each layer i, can be represented by a fourth-order Laplacian tensor $\mathbf{L} \in \mathbb{R}^M \times \mathbb{R}^N \times \mathbb{R}^M \times \mathbb{R}^N$ defined as*

$$\mathbf{L} = \mathbf{D} - \mathbf{A}, \tag{17}$$

where $\mathbf{A}$ is the adjacency tensor and $\mathbf{D}$ is the degree tensor.

The Laplacian tensor can be useful to analyze propagation processes such as diffusion or random walk [10]. Both adjacency and Laplacian tensors are important algebraic representations of the multilayer networks depending on datasets and user objectives. For both directed and undirected layered graphs, we can use the adjacency tensor as the general algebraic representation unless otherwise clarified.

C. Flattening and Analysis

In this part, we introduce the flattening of the multilayer network, which could simplify some operations in the tensor-based M-GSP.

For a multilayer network $\mathcal{M} = \{\mathcal{V}, \mathcal{L}, \mathbf{A}\}$ with M layers and N nodes in each layer, its fourth-order representing tensor $\mathbf{A} \in \mathbb{R}^M \times \mathbb{R}^N \times \mathbb{R}^M \times \mathbb{R}^N$ can be flattened into a second-order matrix to capture the overall edge weights. There are two main flattening schemes in the sense of entities and layers, respectively:

- Layer-wise Flattening: The representing tensor $\mathbf{A} \in \mathbb{R}^M \times \mathbb{R}^N \times \mathbb{R}^M \times \mathbb{R}^N$ can be flattened into a matrix $\mathbf{A}_{FL} \in \mathbb{R}^{MN} \times \mathbb{R}^{MN}$ with each element

$$[A_{FL}]_{N(\alpha-1)+i,N(\beta-1)+j} = A_{\alpha i \beta j}. \tag{18}$$

- Entity-wise Flattening: The representing tensor $\mathbf{A} \in \mathbb{R}^M \times \mathbb{R}^N \times \mathbb{R}^M \times \mathbb{R}^N$ can be flattened into a matrix $\mathbf{A}_{FN} \in \mathbb{R}^{NM} \times \mathbb{R}^{NM}$ with each element

$$[A_{FN}]_{M(i-1)+\alpha,M(j-1)+\beta} = A_{\alpha i \beta j}. \tag{19}$$

These two flattening methods provide two ways to interpret the network structure. In the first method, the flattened multilayer network has M clusters with N nodes in each cluster. The nodes in the same cluster have the same function (belong to the same layer). In the second method, the flattened network has N clusters with M nodes in each cluster. Here, the nodes in the same cluster are from the same entity. Examples of the tensor flattening of a two-layer network with 3 nodes in each layer are shown in Fig. 4. From the examples, we can see that the diagonal blocks in $\mathbb{R}^N \times \mathbb{R}^N$ are the intralayer connections for each layer and other blocks describe the interlayer connections through *layer-wise flattening*; and the diagonal block in $\mathbb{R}^M \times \mathbb{R}^M$ describe the 'intra-entity' connections and other elements represent the 'inter-entity' connections in *entity-wise flattening*. Note that, although the flattened matrix could capture the edge connections of the original representing tensor, the spectral space of the flattened matrix is different from that of representing tensors, which will be further discussed in Section IV-E.

D. Signals and Shifting over the Multilayer Networks

Based on the tensor representation, we define signals and signal shifting over the multilayer networks. In traditional GSP, each signal sample is the attribute of one node. Typically, a graph signal can be represented by a N-length vector for a graph with N nodes. Recall that in traditional GSP, basic signal shifting is defined as Eq. (2) with the representing matrix as the shifting filter. Thus, in M-GSP, we can also define the signals and signal shifting based on the filter implementation.

In M-GSP, each signal sample is also related to one node in the multilayer network. Intuitively, if there are $K = MN$ nodes in the multilayer network, there are MN signal samples in total. Similar to GSP, we use the representing tensor $\mathbf{A} \in \mathbb{R}^M \times \mathbb{R}^N \times \mathbb{R}^M \times \mathbb{R}^N$ as the basic MLN-filter. Since the input signal and the output signal of the MLN-filter should be consistent, i.e., $\mathbf{s}, \mathbf{s}'$ and $\mathbf{s}''$ should have the same tensor size, we define a special form of M-GSP signals to work with the representing tensor as follows.

Definition 4 (Signals over Multilayer Networks). *For a multilayer network $\mathcal{M} = \{\mathcal{V}, \mathcal{L}, \mathbf{A}\}$, with $|\mathcal{L}| = M$ layers and*
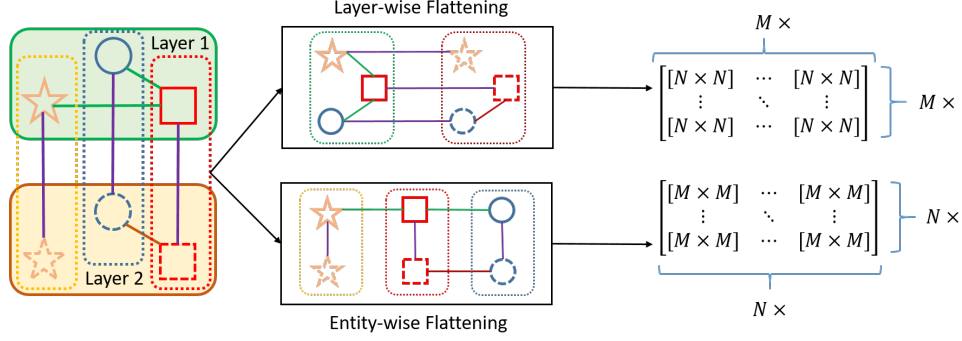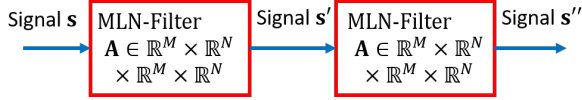
Fig. 4. Example of Multilayer Network Flattening.

Fig. 5. Example of Multilayer Network Filters.

$|l_i| = N$ nodes in each layer i, an alternative definition of multilayer network signals is a second-order tensor

$$\mathbf{s} = (s_{\alpha i}) \in \mathbb{R}^M \times \mathbb{R}^N, \quad 1 \le \alpha \le M, 1 \le i \le N, \quad (20)$$

where the entry $s_{\alpha i}$ is the signal sample in the projected node of entity i in layer α.

Note that, if the multilayer network degenerates to a single-layer graph with $M = 1$, the multilayer network signal becomes a N-length vector, which is similar to that in the traditional GSP. Similar to the representing tensor, the tensor signal $\mathbf{s} \in \mathbb{R}^M \times \mathbb{R}^N$ can also be flattened as a vector in $\mathbb{R}^{MN}$ as follows:

- Layer-wise flattening: $\mathbf{s}_L \in \mathbb{R}^{MN}$ whose entries are calculated as

$$[s_L]_{N(\alpha-1)+i} = s_{\alpha i}. \quad (21)$$

- Entity-wise flattening: $\mathbf{s}_N \in \mathbb{R}^{NM}$ whose entries are calculated as

$$[s_N]_{M(i-1)+\alpha} = s_{\alpha i}. \quad (22)$$

Given the definitions of multilayer network signals and filters, we now introduce the definitions of signal shifting in M-GSP. In traditional GSP, the signal shifting is defined as product between signal vectors and represent matrix, i.e., $\mathbf{s}' = \mathbf{A}\mathbf{s}$. Similarly, we define the shifting in the multilayer network based on the contraction (inner product) between the representing tensor and tensor signals.

Definition 5 (Signal Shifting over Multilayer Networks). *Given the representing matrix $\mathbf{A} \in \mathbb{R}^M \times \mathbb{R}^N \times \mathbb{R}^M \times \mathbb{R}^N$ and the tensor signal $\mathbf{s} \in \mathbb{R}^M \times \mathbb{R}^N$ defined over a multilayer network $\mathcal{M}$, the signal shifting is defined as the contraction (inner product) between $\mathbf{A}$ and $\mathbf{s}$ in one entity-related order and one layer-related order, i.e.,*

$$\mathbf{s}' = \mathbf{A} \diamond \mathbf{s} \in \mathbb{R}^M \times \mathbb{R}^N, \quad (23)$$

where $\diamond$ is the contraction between $\mathbf{A}$ and $\mathbf{s}$ in order three and four. The elements in shifted signal $\mathbf{s}'$ are

$$s'_{\alpha i} = \sum_{\beta=1}^{M} \sum_{j=1}^{N} A_{\alpha i \beta j} s_{\beta j}. \quad (24)$$

From Eq. (24), there two important factors to construct the shifted signal: 1) The signal in the neighbors of the node $v_{\alpha i}$; and 2) The intensity of interactions between the node $v_{\alpha i}$ and its neighbors. Then, the signal shifting is related to the diffusion process over the multilayer networks. More specifically, if $\mathbf{A}$ is the adjacency tensor, signals shift in directions of edges. To better illustrate the signal shifting based on the representing tensor, we use a two-layer directed network shown in Fig. 6 as an example. In this multilayer network, the original signal $\mathbf{s}$ is defined as

$$\mathbf{s} = \begin{bmatrix} 1 & 2 & 3 \\ 6 & 5 & 4 \end{bmatrix}, \quad (25)$$

and the adjacency tensor $\mathbf{A}$ is defined as

$$\mathbf{A}_{(1,:,1,:)} = \begin{bmatrix} 0 & 0 & 0 \\ 1 & 0 & 0 \\ 0 & 1 & 0 \end{bmatrix}, \mathbf{A}_{(2,:,2,:)} = \begin{bmatrix} 0 & 1 & 0 \\ 0 & 0 & 1 \\ 0 & 0 & 0 \end{bmatrix},$$

$$\mathbf{A}_{(2,:,1,:)} = \begin{bmatrix} 0 & 0 & 0 \\ 0 & 0 & 0 \\ 0 & 0 & 1 \end{bmatrix}, \mathbf{A}_{(1,:,2,:)} = \begin{bmatrix} 1 & 0 & 0 \\ 0 & 0 & 0 \\ 0 & 0 & 0 \end{bmatrix},$$

for each fiber. Then, the shifted signal is calculated as

$$\mathbf{s}' = \begin{bmatrix} 6 & 1 & 2 \\ 5 & 4 & 3 \end{bmatrix}. \quad (26)$$

From Eq. (26), we can see that the signal shift one step following the direction of the links.

For the flattened signal and the flattened adjacency tensor, the shifted signals are represented as $\mathbf{s}'_{FL} = \mathbf{A}_{FL} \cdot \mathbf{s}_{FL} \in \mathbb{R}^{MN}$ for layer-wise flattening; and $\mathbf{s}'_{FN} = \mathbf{A}_{FN} \cdot \mathbf{s}_{FN} \in \mathbb{R}^{NM}$ for entity-wise flattening.

E. Multilayer Network Spectral Space

We now provide the definitions of spectral space of the multilayer network based on the tensor representation. In traditional GSP, graph Fourier (spectral) space is defined according to the eigenspace of the representing matrix [2]. Similarly, we define the MLN spectral space based on the decomposition of the representing tensor.
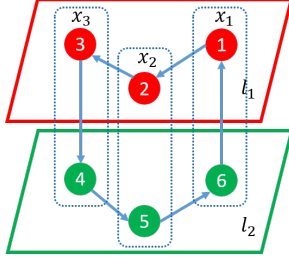
Fig. 6. Example of Multilayer Network Shifting.

1) Eigen-Tensor of Undirected Multilayer Networks: To define the spectral (Fourier) space of the multilayer network, we start from the undirected multilayer network. For a multilayer network $\mathcal{M} = \{\mathcal{V}, \mathcal{L}, \mathbf{A}\}$ with M layers and N nodes, the eigen-tensor $\mathbf{V} \in \mathbb{R}^M \times \mathbb{R}^N$ of the representing tensor is defined in the tensor-based multilayer network theory [10] as

$$\mathbf{A} \diamond \mathbf{V} = \lambda \mathbf{V}. \tag{27}$$

Next, we show how to obtain the eigen-tensors and the approximated factorization from the representing tensor. In an undirected multilayer network, the representing tensor (adjacency/Laplacian) $\mathbf{A}$ is partially symmetric between orders one and three, and between orders two and four, respectively. Then, the representing tensor can be written with the consideration of the multilayer network structure as follows:

$$\mathbf{A} \approx \sum_{\alpha=1}^{M} \sum_{i=1}^{N} \lambda_{\alpha i} \cdot \mathbf{f}_\alpha \circ \mathbf{e}_i \circ \mathbf{f}_\alpha \circ \mathbf{e}_i \tag{28}$$

$$= \sum_{\alpha=1}^{M} \sum_{i=1}^{N} \lambda_{\alpha i} \mathbf{V}_{\alpha i} \circ \mathbf{V}_{\alpha i} \tag{29}$$

$$= \sum_{k=1}^{MN} \lambda_k \mathbf{V}_k \circ \mathbf{V}_k, \tag{30}$$

where $\mathbf{f}_\alpha \in \mathbb{R}^M$ are orthonormal, $\mathbf{e}_i \in \mathbb{R}^N$ are orthonormal and $\mathbf{V}_{\alpha i} = \mathbf{f}_\alpha \circ \mathbf{e}_i \in \mathbb{R}^M \times \mathbb{R}^N$.

Note that, if there is only one layer in the multilayer network, Eq. (28) reduces to the eigendecomposition of a normal single-layer graph, i.e.,

$$\mathbf{A} = \sum_{i=1}^{N} \lambda_i \mathbf{e}_i \circ \mathbf{e}_i \tag{31}$$

$$= [\mathbf{e}_1 \cdots \mathbf{e}_N] \begin{bmatrix} \lambda_1 & \cdots & 0 \\ \vdots & \ddots & \vdots \\ 0 & \cdots & \lambda_N \end{bmatrix} \begin{bmatrix} \mathbf{e}_1^{\mathrm{T}} \\ \vdots \\ \mathbf{e}_N^{\mathrm{T}} \end{bmatrix}. \tag{32}$$

We now have the following property of $\mathbf{V}_{\alpha i}$.

Property 1. *The factor tensor $\mathbf{V}_{\alpha i}$ of the representing tensor $\mathbf{A}$ is the approximated eigen-tensor of $\mathbf{A}$.*

Proof. Suppose that $\mathbf{V}_{\alpha i}$ is one factor tensor of $\mathbf{A}$ obtained from Eq. (28).

Let $\delta[k]$ denote the Kronecker impulse. Since $\mathbf{f}_\alpha$ forms an orthonormal basis, then the inner product would satisfy

$$< \mathbf{f}_\alpha, \mathbf{f}_\beta >= \sum_k [f_\alpha]_k \cdot [f_\beta]_k = \delta[\alpha - \beta].$$

Similarly,

$$< \mathbf{e}_i, \mathbf{e}_j >= \delta[i - j].$$

$$\mathbf{A} \diamond \mathbf{V}_{\alpha i} = \sum_{\sigma=1}^{M} \sum_{k=1}^{N} A_{\beta j \sigma k} [V_{\alpha i}]_{\sigma k} \tag{33}$$

$$\approx \sum_{\sigma=1}^{M} \sum_{k=1}^{N} \sum_{\gamma=1}^{M} \sum_{t=1}^{N} \lambda_{\gamma t} [f_\gamma]_\beta [e_t]_j [f_\gamma]_\sigma [e_t]_k [V_{\alpha i}]_{\sigma k}. \tag{34}$$

Then, we have

$$\sum_{\sigma=1}^{M} \sum_{k=1}^{N} [f_\gamma]_\sigma [e_t]_k [V_{\alpha i}]_{\sigma k} = \sum_{\sigma=1}^{M} \sum_{k=1}^{N} [f_\gamma]_\sigma [e_t]_k [f_\alpha]_\sigma [e_i]_k$$

$$= \sum_{\sigma=1}^{M} [f_\gamma]_\sigma [f_\alpha]_\sigma \sum_{k=1}^{N} [e_t]_k [e_i]_k$$

$$=< \mathbf{f}_\gamma, \mathbf{f}_\alpha > \cdot < \mathbf{e}_t, \mathbf{e}_i >$$

$$= \delta[\gamma - \alpha] \delta[t - i] \tag{35}$$

Thus,

$$\mathbf{A} \diamond \mathbf{V}_{\alpha i} = \lambda_{\alpha i} \mathbf{V}_{\alpha i}, \tag{36}$$

which indicates that $\mathbf{V}_{\alpha i}$ is the approximated eigen-tensor. $\quad\square$

Similar to the traditional GSP where the graph Fourier space is defined by the eigenvectors of the representing matrix, we define the MLN Fourier space as follows.

Definition 6 (Multilayer Network Fourier Space). *For a multilayer network $\mathcal{M} = \{\mathcal{V}, \mathcal{L}, \mathbf{A}\}$ with M layers and N nodes, the MLN spectral (Fourier) space is defined as the space consisting of all spectral tensors $\{\mathbf{V}_1, \cdots, \mathbf{V}_{MN}\}$, which characterizes the joint features of entities and layers. Moreover, the tensor factorization $\{\mathbf{f}_1, \cdots, \mathbf{f}_M\}$ and $\{\mathbf{e}_1, \cdots, \mathbf{e}_N\}$ characterize each layer and entity, respectively.*

With the definition of the MLN Fourier space, we now explore the properties of the MLN spectral tensors. We first introduce the orthogonality of the spectral tensor as follows.

Property 2. *Let $\mathbf{U}_1$ be the contraction of $\mathbf{V}$ in the layer dimension, i.e., $\mathbf{U}_1 = \mathbf{V}_{\alpha i}^{\mathrm{T}} \mathbf{V}_{\beta j}$, and $\mathbf{U}_2$ be the contraction of $\mathbf{V}$ in the entity dimension, i.e., $\mathbf{U}_2 = \mathbf{V}_{\alpha i} \mathbf{V}_{\beta j}^{\mathrm{T}}$, then we have the following properties*

- $\mathbf{U}_1 = \mathbf{e}_i \circ \mathbf{e}_j \cdot \delta[\alpha - \beta]$;
- $\mathbf{U}_2 = \mathbf{f}_\alpha \circ \mathbf{f}_\beta \cdot \delta[i - j]$.

This property can be easily obtained with the inner product in different orders separately. We are more interested to generalize the orthogonality of the spectral tensor into a similar definition of matrix. By constructing a fourth-order tensor $\mathbf{U} \in \mathbb{R}^M \times \mathbb{R}^N \times \mathbb{R}^M \times \mathbb{R}^N$ with $\mathbf{V}_{\alpha i}$ as its elements, i.e.,

$$U_{\alpha i \beta j} = [V_{\alpha i}]_{\beta j}, \tag{37}$$

we can have the following property.

Property 3. *Let $\mathbf{W} = \mathbf{U} \otimes \mathbf{U}$ where $W_{\alpha i \beta j} = \sum_{p,\theta} U_{\beta j \theta p} \times U_{\alpha i \theta p}$. Then, $\mathbf{W}$ is super-diagonal with super-diagonal elements all equal to one.*

Proof. Let $\mathbf{V}_k = \mathbf{V}_{\alpha i} = \mathbf{f}_\alpha \circ \mathbf{e}_i$ and $\mathbf{V}_t = \mathbf{V}_{\beta j} = \mathbf{f}_\beta \circ \mathbf{e}_j$. Then, we have

$$
\begin{aligned}
W_{\alpha i \beta j} &= \sum_{\theta, p} [V_k]_{\theta p} [V_t]_{\theta p} \\
&= \sum_p [e_i]_p [e_j]_p \sum_\theta [f_\alpha]_\theta [f_\beta]_\theta \\
&= <\mathbf{f}_\alpha, \mathbf{f}_\beta > \cdot <\mathbf{e}_i, \mathbf{e}_j>, \\
&= \delta[\alpha - \beta] \delta[i - j].
\end{aligned} \tag{38}
$$

$\square$

In Property 3, if the undirected multilayer network degrades to the normal graph, $\mathbf{W} = \mathbf{U} \otimes \mathbf{U} = \mathbf{U}^\mathrm{T} \mathbf{U} = \mathbf{I}$, where $\mathbf{U} = [\mathbf{e}_1 \cdots \mathbf{e}_N]$ contains all the eigenvectors in columns.

After analyzing the tensor-based properties of the spectrum in the multilayer networks, now we implement the flattening analysis of the spectral tensors.

Property 4. *The two types of flattened tensor in Eq. (21) and Eq. (22) lead to the same eigenvalues.*

Proof. Suppose $(\lambda, \mathbf{x})$ is an eigenpair of $\mathbf{A}_{FL}$, i.e.,

$$
\mathbf{A}_{FL} \cdot \mathbf{x} = \lambda \mathbf{x}. \tag{39}
$$

Let $x_{N(\alpha-1)+i} = y_{M(i-1)+\alpha}$. Since

$$
\begin{aligned}
A_{\alpha i \beta j} &= [A_{FL}]_{N(\alpha-1)+i, N(\beta-1)+j} \\
&= [A_{FN}]_{M(i-1)+\alpha, M(j-1)+\beta},
\end{aligned} \tag{40}
$$

we have

$$
\mathbf{A}_{FN} \cdot \mathbf{y} = \lambda \mathbf{y}. \tag{41}
$$

Thus, λ is also an eigenvalue of $\mathbf{A}_{FN}$. $\square$

This property shows that the flattened tensors are the reshape of the original representing tensor, and could capture some of the spectrum properties as follows.

Property 5. *Given the eigenpair $(\lambda_{FL}, \mathbf{x})$ of the layer-wise flattened tensor, the eigenpair $(\lambda, \mathbf{V})$ of the original adjacency tensor can be calculated as*

$$
\lambda = \lambda_{FL}, \tag{42}
$$

$$
V_{\alpha i} = x_{N(\alpha-1)+i}. \tag{43}
$$

Similarly, given the eigenpair $(\lambda_{FN}, \mathbf{y})$ of the entity-wise flattened tensor, the eigenpair $(\lambda, \mathbf{V})$ of the original adjacency tensor can be calculated as

$$
\lambda = \lambda_{FN}, \tag{44}
$$

$$
V_{\alpha i} = y_{M(i-1)+\alpha}. \tag{45}
$$

The Property 5 shows that we can calculate the eigentensor from the flattened tensor to simplify the decomposition operations. Moreover, since $\mathbf{x}$ and $\mathbf{y}$ are also orthonormal, we have $<\mathbf{V}_{\alpha i}, \mathbf{V}_{\beta j}> = <\mathbf{x}_k, \mathbf{x}_t> = <\mathbf{y}_p, \mathbf{y}_q>$, where k, t and p, q are the related reshaped indices of $\mathbf{V}_{\alpha i}$ and $\mathbf{V}_{\beta j}$, respectively. Thus, we can see that $\mathbf{V}$ acquired from tensor flattening also satisfy the orthogonality requirement of Property 3.

Note that $\mathbf{V}$ from the flattening analysis are not necessarily the ideal case of $\mathbf{V}_{\alpha i} = \mathbf{f}_\alpha \circ \mathbf{e}_i$. If we are interested in the

---

Algorithm 1 Eigen-Tensor Calculation

1: Flatten the adjacency tensor into a supra-matrix;
2: Decompose the supra-matrix into eigenvalues and eigenvectors;
3: Reshape the eigenvectors of the supra-matrix according to the flattening type;
4: Decompose/Approximate eigen-tensors by factorization.

---

properties of the individual orders, we could further implement an approximated decomposition on $\mathbf{V}_{\alpha i} \approx \mathbf{f}_\alpha \circ \mathbf{e}_i$ to obtain the best fitted $\mathbf{f}_\alpha$ and $\mathbf{e}_i$. Thus, in addition to the direct factorization mentioned of Eq. (28), we could approximate the spectrum of the multilayer networks from the flattened supra-matrix (second-order tensor) as in Algorithm 1.

2) Singular-Tensor of Undirected Multilayer Networks: In addition to the eigen-decomposition, the singular value decomposition (SVD) is another important decomposition to factorize a matrix. In this part, we provide the higher-order SVD (HOSVD) of the representing tensor as an alternative definition of spectrum for the multilayer networks.

From Eq. (28), the factorization can be interpreted as a special case of the CP decomposition [25], which decomposes the tensor into a series of spectral vectors. Now consider HOSVD, which is a special case of Tucker decomposition by decomposing the tensor into different fibers [27]. Given the multilayer network $\mathcal{M} = \{\mathcal{V}, \mathcal{L}, \mathbf{A}\}$ with M layers and N nodes in each layer, its representing tensor $\mathbf{A} \in \mathbb{R}^M \times \mathbb{R}^N \times \mathbb{R}^M \times \mathbb{R}^N$ can be decomposed via HOSVD as follows:

$$
\mathbf{A} \approx \mathbf{S} \times_1 \mathbf{U}^{(1)} \times_2 \mathbf{U}^{(2)} \times_3 \mathbf{U}^{(3)} \times_4 \mathbf{U}^{(4)}, \tag{46}
$$

where $\mathbf{U}^{(n)} = [\mathbf{U}_1^{(n)} \quad \mathbf{U}_2^{(n)} \quad \cdots \quad \mathbf{U}_{I_n}^{(n)}]$ is a unitary $(I_n \times I_n)$ matrix, with $I_1 = I_3 = M$ and $I_2 = I_4 = N$. $\mathbf{S}$ is a complex $(I_1 \times I_2 \times I_3 \times I_4)$-tensor of which the subtensor $\mathbf{S}_{i_n}$ obtained by fixing nth index to α have

- $<\mathbf{S}_{i_n=\alpha}, \mathbf{S}_{i_n=\beta}> = 0$ where $\alpha \neq \beta$.
- $||\mathbf{S}_{i_n=1}|| \geq ||\mathbf{S}_{i_n=2}|| \geq \cdots \geq ||\mathbf{S}_{i_n=I_n}|| \geq 0$.

The Frobenius-norms $\sigma_i^{(n)} = ||S_{i_n=i}||$ is the n-mode singular value, and $\mathbf{U}^{(i)}$ are the corresponding n-mode singular vectors. For an undirected multilayer network, the adjacency tensor is symmetric for every 2-D combination. Thus, there are two modes of singular spectrum, i.e., $(\gamma_\alpha, \mathbf{f}_\alpha)$ for mode $1, 3$, and $(\sigma_i, \mathbf{e}_i)$ for mode $2, 4$. More specifically, $\mathbf{U}^{(1)} = \mathbf{U}^{(3)} = (\mathbf{f}_\alpha)$ and $\mathbf{U}^{(2)} = \mathbf{U}^{(4)} = (\mathbf{e}_i)$. Since the joint singular tensor captures the consistent information of entities and layers, it can be calculated as

$$
(\lambda_{\alpha i}, \mathbf{V}_{\alpha i}) = (\gamma_\alpha \cdot \sigma_i, \mathbf{f}_\alpha \cdot \mathbf{e}_i). \tag{47}
$$

Note that the diagonal entries of $\mathbf{S}$ are not the eigenvalues or frequency coefficients of the adjacency tensor in general. The multilayer network singular space is defined as follows.

Definition 7 (Multilayer Network Singular Space). *For a multilayer network $\mathcal{M} = \{\mathcal{V}, \mathcal{L}, \mathbf{A}\}$ with M layers and N nodes, the MLN singular space is defined as the space consisting of all singular tensors $\{\mathbf{V}_1 \cdots \mathbf{V}_{MN}\}$ obtained from Eq. (47). The singular vectors $\{\mathbf{f}_1, \cdots, \mathbf{f}_M\}$ and $\{\mathbf{e}_1, \cdots, \mathbf{e}_N\}$ in Eq. (46) characterize layers and entities, respectively.*

Compared to the eigen-tensors in Eq. (28), the singular tensors come from the combinations of the singular vectors, thus are capable of capturing information of layers and entities more efficiently. Eigen-decomposition, however, focuses more on the joint information and approximate the separate information of layers and entities. We shall provide further discussion on the performance of different decomposition methods in Section IV-C and Part II of this two-part paper [21].

3) Spectral Space of Directed Multilayer Networks: Unlike for undirected graphs, representing tensors of directed graphs is asymmetric, thereby making each layer or entity characterized by a pair of spectral vectors. To find the spectral space of a directed multilayer network, we also present two ways to compute: 1) Flattening analysis; and 2) Tensor factorization:

- *Flattening analysis:* Similar to the representing tensor of undirected graphs, we flatten the representing tensor as a second-order supra-matrix, and define spectral space as the reshape of the eigenvectors of the supra-matrix. The flattened matrix $\mathbf{A}_{FX}$ (or $\mathbf{A}_{FN}$, $\mathbf{A}_{FL}$) can be decomposed as

$$\mathbf{A}_{FX} \approx \mathbf{E}\Sigma\mathbf{E}^{-1}, \tag{48}$$

where $\mathbf{E} \in \mathbb{R}^{MN} \times \mathbb{R}^{MN}$ is the matrix of eigenvectors and $\Sigma = diag(\lambda_i)$ is a diagonal matrix of eigenvalues. Then, we can reshape the eigenvectors, i.e., each column of $\mathbf{E}$ as $\mathbf{V}_k \in \mathbb{R}^M \times \mathbb{R}^N$, and reshape each row of $\mathbf{E}^{-1}$ as $\mathbf{U}_k \in \mathbb{R}^M \times \mathbb{R}^N$. Consequently, the original tensor can decomposed into

$$\mathbf{A} \approx \sum_{k=1}^{MN} \lambda_k \mathbf{V}_k \circ \mathbf{U}_k. \tag{49}$$

- *Tensor Factorization*: We can also compute the spectrum from the tensor factorization based on CP-decomposition

$$\mathbf{A} \approx \sum_{k=1}^{R} \lambda_k \mathbf{a}_k \circ \mathbf{b}_k \circ \mathbf{c}_k \circ \mathbf{d}_k \tag{50}$$

$$= \sum_{k=1}^{R} \lambda_k \mathbf{V}_k \circ \mathbf{U}_k. \tag{51}$$

where R is the rank of tensor, $\mathbf{a}_k, \mathbf{c}_k \in \mathbb{R}^M$ characterize layers, $\mathbf{b}_k, \mathbf{d}_k \in \mathbb{R}^N$ characterize entities, and $\mathbf{V}_k = \mathbf{a}_k \circ \mathbf{b}_k, \mathbf{U}_k = \mathbf{c}_k \circ \mathbf{d}_k \in \mathbb{R}^M \times \mathbb{R}^N$ characterize the joint features. Since there are MN nodes, it is clear that $R \le MN$. Note that, for a single layer, Eq. (50) reduces to

$$\mathbf{A} \approx \sum_{k=1}^{N} \lambda_k \mathbf{v}_k \circ \mathbf{u}_k. \tag{52}$$

Moreover, if $\mathbf{V} = (\mathbf{v}_k)$ and $\mathbf{U} = (\mathbf{u}_k^{\mathrm{T}}) = \mathbf{V}^{-1}$ are orthogonal bases, Eq. (52) is in a consistent form of the eigendecomposition in a single-layer normal graph. In addition, Eq. (28) is also a special case of Eq. (50) if the multilayer network is undirected.

Since tensor decomposition is less stable when exploring the factorization of a specific order or when extracting the separate features in the asymmetric tensors, we will mainly focus on

spectrum properties of undirected multilayer networks in the remaining of the two-part series for simplicity and clarity of presentation. Although some properties in undirected networks still apply to directed networks, we shall defer more general analysis of directed networks to future works.

F. Graph Fourier Transform (GFT) and Graph Singular-Value Transform (GST) in Undirected Multilayer Networks

From the definitions of the MLN spectral space and singular space, we are ready to define multilayer network graph Fourier transform (M-GFT) and multilayer network singular value transform (M-GST). Recall that in GSP, the GFT is defined based on the inner product of $\mathbf{V}^{-1}$ and the signals $\mathbf{s}$ defined in Eq. (4). Similarly, we can define the M-GFT based on the spectral tensors of the adjacency tensor $\mathbf{A}$.

Definition 8 (M-GFT). *Let $\mathbf{U}_f = (\mathbf{V}_{\alpha i}) \in \mathbb{R}^M \times \mathbb{R}^N \times \mathbb{R}^M \times \mathbb{R}^N$ consist of the spectral tensors of the representing tensor $\mathbf{A}$, where*

$$[U_f]_{\alpha i \beta j} = [V_{\alpha i}]_{\beta j}. \tag{53}$$

The M-GFT can be defined as the contraction between $\mathbf{U}_f$ and the tensor signal $\mathbf{s} \in \mathbb{R}^M \times \mathbb{R}^N$, i.e.,

$$\hat{\mathbf{s}} = \mathbf{U}_f \diamond \mathbf{s}. \tag{54}$$

Each element of $\hat{\mathbf{s}}$ in Eq. (54) can be calculated as

$$\hat{s}_{\alpha i} = \sum_{\beta, j} [U_f]_{\alpha i \beta j} s_{\beta j} \tag{55}$$

$$= \sum_{\beta, j} [V_{\alpha i}]_{\beta j} s_{\beta j} \tag{56}$$

$$= \sum_{\beta, j} [f_\alpha]_\beta \cdot [e_i]_j \cdot s_{\beta j}. \tag{57}$$

Let $\mathbf{F}_f = [\mathbf{f}_1 \cdots \mathbf{f}_M] \in \mathbb{R}^M \times \mathbb{R}^M$ and $\mathbf{E}_f = [\mathbf{e}_1 \cdots \mathbf{e}_N] \in \mathbb{R}^N \times \mathbb{R}^N$. We then have

$$\tilde{\mathbf{s}} = \mathbf{F}_f^{\mathrm{T}} \mathbf{s} \mathbf{E}_f, \tag{58}$$

with each element $\tilde{s}_\alpha = \sum_{j,\beta} [f_\alpha]_\beta \cdot [e_i]_j \cdot s_{\beta j}$. Clearly, the M-GFT can be obtained via

$$\hat{\mathbf{s}} = \tilde{\mathbf{s}} = \mathbf{F}_f^{\mathrm{T}} \mathbf{s} \mathbf{E}_f. \tag{59}$$

Then, we have the following definition of order-wise M-GFT to capture the features of layers and entities separately.

Definition 9 (Order-wise M-GFT). *Given the spectral vectors $\mathbf{F}_f = [\mathbf{f}_1 \cdots \mathbf{f}_M] \in \mathbb{R}^M \times \mathbb{R}^M$ and $\mathbf{E}_f = [\mathbf{e}_1 \cdots \mathbf{e}_N] \in \mathbb{R}^N \times \mathbb{R}^N$, the layer-wise M-GFT can be defined as*

$$\hat{\mathbf{s}}_L = \mathbf{F}_f^{\mathrm{T}} \mathbf{s} \in \mathbb{R}^M \times \mathbb{R}^N, \tag{60}$$

and the entity-wise M-GFT can be defined as

$$\hat{\mathbf{s}}_N = \mathbf{s} \mathbf{E}_f \in \mathbb{R}^M \times \mathbb{R}^N. \tag{61}$$

If there is only one layer in the multilayer network, the M-GFT calculated with $\mathbf{s}^T \in \mathbb{R}^N$ as

$$(\hat{\mathbf{s}}_N)^{\mathrm{T}} = (\mathbf{s}\mathbf{E}_f)^{\mathrm{T}} \in \mathbb{R}^N, \tag{62}$$

has the same form as the traditional GFT in Eq. (4).

In addition, since $\mathbf{f}_\alpha$ and $\mathbf{e}_i$ are orthonormal basis of undirected multilayer networks, the inverse M-GFT can be calculated as

$$\mathbf{s}' = \mathbf{F}_f \hat{\mathbf{s}} \mathbf{E}_f^\mathrm{T}. \tag{63}$$

Similar to M-GFT, we can define the M-GST based on the singular tensors.

Definition 10 (M-GST). *Suppose that* $\mathbf{U}_s = (\mathbf{f}_\alpha \circ \mathbf{e}_i) \in \mathbb{R}^M \times \mathbb{R}^N \times \mathbb{R}^M \times \mathbb{R}^N$ *consists of the singular vectors of the representing tensor* $\mathbf{A}$ *in Eq. (46), where*

$$[U_s]_{\alpha i \beta j} = [f_\alpha]_\beta \cdot [e_i]_j. \tag{64}$$

The M-GST can be defined as the contraction between $\mathbf{U}_s$ *and the tensor signal* $\mathbf{s} \in \mathbb{R}^M \times \mathbb{R}^N$, *i.e.,*

$$\check{\mathbf{s}} = \mathbf{U}_s \diamond \mathbf{s}. \tag{65}$$

If the singular vectors is included in $\mathbf{F}_s = [\mathbf{f}_1 \cdots \mathbf{f}_M] \in \mathbb{R}^M \times \mathbb{R}^M$ *and* $\mathbf{E}_s = [\mathbf{e}_1 \cdots \mathbf{e}_N] \in \mathbb{R}^N \times \mathbb{R}^N$, *the layer-wise M-GST can be defined as*

$$\check{\mathbf{s}}_L = \mathbf{F}_s^\mathrm{T} \mathbf{s} \in \mathbb{R}^M \times \mathbb{R}^N, \tag{66}$$

and the entity-wise M-GST can be defined as

$$\check{\mathbf{s}}_N = \mathbf{s} \mathbf{E}_s \in \mathbb{R}^M \times \mathbb{R}^N. \tag{67}$$

Similarly, the inverse M-GST can be defined in the same way as Eq. (63) with the unitary $\mathbf{F}_s$ and $\mathbf{E}_s$.

G. Spectrum Ranking in the Multilayer Network

In traditional GSP, the eigenvalues correspond to graph frequencies, whereas the total variation is an alternative measurement of the order of the graph frequencies. Similarly, we use the total variation of $\lambda_{\alpha i}$ based on the spectral tensors to rank the MLN frequencies. In M-GSP, the total variation is defined as follows:

$$TV(\lambda_{\alpha i}) = ||\mathbf{V}_{\alpha i} - \frac{1}{|\lambda|_{max}} \mathbf{A} \diamond \mathbf{V}_{\alpha i}||_k \tag{68}$$

$$= |1 - \frac{\lambda}{|\lambda|_{max}}| \cdot ||V_{\alpha i}||_k. \tag{69}$$

Here, $||\cdot||_k$ could be designed depending on the applications. For example, the l_2 norm could be efficient in denoising and signal smoothing [2]. The graph frequency related to $\lambda_{\alpha i}$ is said to be a higher frequency if its total variation $TV(\lambda_{\alpha i})$ is larger, and its corresponding spectral tensor $\mathbf{V}_{\alpha i}$ is a higher frequency spectrum. We shall provide more details on interpretation of MLN frequency in Section IV-A.

IV. Discussions and Interpretive Insights

In this section, we focus on the insights and physical meaning of frequency to help interpret the MLN spectral space. In addition, we provide some numerical results and examples of the M-GSP.
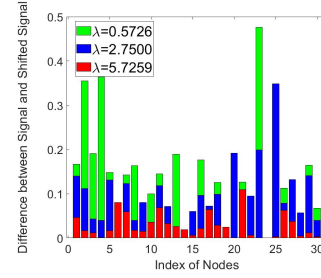

Fig. 7. Example of MLN Frequencies.

TABLE I
TOTAL DIFFERENCE OF ALL NODES

Eigenvalue	0.5726	2.7500	5.7259
Total Differences	3.7439	2.6846	0.8293

A. Interpretation of M-GSP Frequency

We are interested in an intuitive interpretation of the MLN frequencies. In Eq. (68), the MLN frequency is defined based on the total variation of the spectral tensors.

To better understand its physical meaning, we start with the total variation in digital signal processing (DSP). The total variation in DSP is defined as differences among signals over time [34]. Moreover, the total variations of frequency components have a 1-to-1 correspondence to frequencies in the order of their values. If the total variation of a frequency component is larger, the corresponding frequency with the same index is higher. This means that, a higher frequency component changes faster over time and exhibits a larger total variation. Interesting readers are referred to the related sections in [2] and [8] for a detailed explanation of the total variation and frequency in DSP.

Now, return to M-GSP. Given spectral tensors $\mathbf{V}_k \in \mathbb{R}^M \times \mathbb{R}^N$ of a multilayer network, a signal $\mathbf{s} \in \mathbb{R}^M \times \mathbb{R}^N$ can be written in a weighted sum of the spectrum, i.e.,

$$\mathbf{s} = \sum_k a_k \mathbf{V}_k. \tag{70}$$

Viewing the spectral tensor as a signal component, the total variation is in the form of differences between the original signal and its shifted version in Eq. (68). If the signal component shifts faster over the multilayer network, the corresponding total variation is larger. Since we relate higher frequency component with a larger total variation, the MLN frequency indicates how fast the signal propagates over the multilayer network. If a signal $\mathbf{s}$ contains more high frequency components, it shifts faster in the given topology of the multilayer network. Here, we use an example to illustrate it further. We construct a multiplex network with six layers and five nodes in each layer based on the $Erd\ddot{o}s - R\dot{e}nyi$ (ER) random graphs [35]. Each node has a probability of 30% to connect other nodes for intralayer connections and its counterparts in other layers for interlayer connections. We use the Laplacian tensor as representing tensor and l_1-norm of the flattened signal to calculate the total variation. Then we have $\lambda_k \geq 0$ and $TV(\lambda_k) = |1 - \frac{\lambda}{\lambda_{max}}|$ for $1 \leq k \leq MN$. Clearly, the total variation is larger if the eigenvalue is smaller, i.e., smaller eigenvalues correspond to higher frequencies.
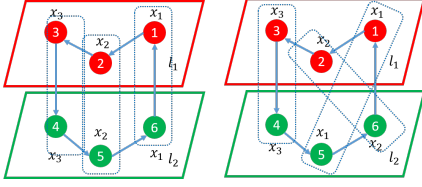
Fig. 8. Example of Different Entities.

TABLE II
ERROR OF DECOMPOSING THE REPRESENTING TENSOR

Graph Structure	ER(0.3,0.3,6,5)	ER(0.5,0.7,11,15)	ER(0.8,0.7,6,15)
Eigen-tensor	8.3893e-15	1.6001e-13	3.8347e-13
HOSVD	1.011e-14	1.9563e-13	1.9056e-13
OPT-CP	9.22e-01	8.82e-01	9.24e-01
Tucker	9.37e-05	9.10e-05	9.40e-05

We next evaluate the differences between shifted signal and original signal by treating different eigen-tensor as signals. From the results given in Fig. 7, the shifted signal sample of each node changes more compared to its original samples. Also from the results given n Table I, we can see that a higher frequency signal component exhibits a larger total difference between the original signal and its shifts, indicating a faster propagation over the multilayer network.

B. Interpretation of Entities and Layers

To gain better physical insight of entities and layers, we discuss two categories of datasets:

- In most of the physical systems and datasets, signals can be modeled with a specific physical meaning in terms of layers and entities. In smart grid, for example, each entity can be a station, connected over two layers of computation and power transmission, respectively. Another example is video. By modeling each pixel as an entity and a video frame as a layer, each node represents the observed (value) of the pixel in certain video frame. M-GSP can be intuitive tool for signal processing over these datasets and systems.
- In some scenarios, however, the datasets usually only has a definition of layers without meaningful entities. Especially, for multilayer networks with different numbers of nodes, we need to inject some isolated nodes to augment the multilayer network. Often in such applications, it is hard to identify the physical meaning of entities. Here, the entities may be virtual and are embedded in the underlying structure of the multilayer network. Although definition of a virtual entity may vary with the chosen adjacency tensor, it relates to the topological structure in terms of global spectral information. For example, in Fig. 8, we can use two different definitions of virtual entities. Although the representing tensors of these two definitions differ, their eigenvalues remain the same. Considering also layer-wise flattening, the two supramatrices are related by reshaping, by exchanging the fourth and fifth columns and rows. They also have the same eigenvalues, whereas the eigentensors can also be the same by implementing the reshaping operations. Note that, if we are interested in capturing distinct information
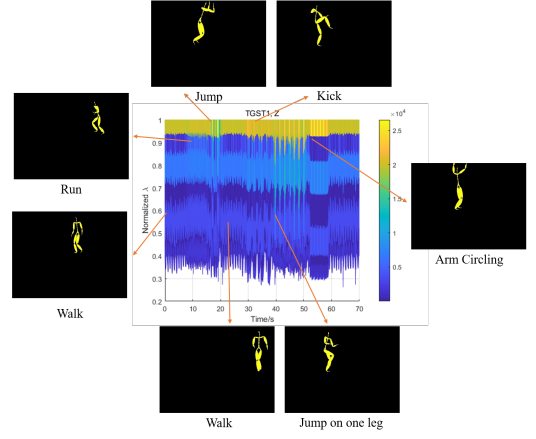

Fig. 9. Example of Transformed Signals in a Dynamic Point Cloud.

from entities, their spectra would change with different definitions of virtual entities.

C. Comparison of Different Decomposition Methods

To compare the accuracy in recovering the representing tensor using different tensor decomposition methods we examine eigen-tensor decomposition, HOSVD, optimal CP decomposition and Tucker decomposition in the ER random graph $ER(p,q,M,N)$, where M is the number of layers with N nodes in each layer, p is the intralayer connection probability and q is the interlayer connection probability. We apply different decomposition methods of similar complexity, and compute errors between the decomposed and the original tensors. From the results of Table II, we can see that the eigen-tensor decomposition and HOSVD exhibit better overall accuracy. Generally, eigen-tensor decomposition is more suitable for applications emphasizing joint features of layers and entities. On the other hand, HOSVD is more efficient in separating individual features of layers and entities. Note that, here we only used recovery accuracy to measure different decompositions. However, different decompositions may have different performance advantages when capturing different data features that can be measured with different metrics. We will provide more results on realistic datasets in Part II [21] of this two-part series.

D. Example of Transformed Signal in Real Dataset

In this part, we provide an example of the transformed signal based on the M-GST.

Spectral analysis of signals is one of the basic tools in data analysis. Here, we propose a short time M-GST method to analyze dynamic point cloud. Given a dynamic point cloud with M frames and at most N points in each frame, we model it as a multilayer network with M layers and N nodes in each layer. More specifically, we test the singular spectrum analysis over the motion sequences of subject 86 in the CMU database [36]. To implement the M-GST, we first divide the motion sequence into several shorter sequences with N_f frames. Next for each shorter sequence, we model interlayer connections by connecting points with the same label among successive frames. For points in the same frame, we connect two points

based on the Gaussian-kernel within an Euclidean threshold τ_s [6]. Let $\mathbf{x}_i$ be the 3D coordinates of the ith point. We assign an edge weight between two points $\mathbf{x}_i$ and $\mathbf{x}_j$ as a nonzero $A_{i,j} = \exp(-\|\mathbf{x}_i - \mathbf{x}_j\|_2^2/\sigma^2)$ only if $\|\mathbf{x}_i - \mathbf{x}_j\|_2^2 \leq \tau_s$. Next, we estimate the spatial and temporal basis vectors of each shorter-term sequences by HOSVD in Eq. (46) [37]. Finally, we use the 3D coordinates of all points in each shorter-term sequences as signals and calculate their M-GST. To illustrate the results of M-GST, we examine the spectrogram similar to that of short-time Fourier transform (STFT) [38]. In Fig. 9, we transform the signal defined by the coordinates in Z dimension via M-GST, and plot the transformed results for the divided frame sequence. From the results, we can easily identify the different types of motions based on the MLN singular analysis.

The above case is only one simple example of spectrum analysis within the M-GSP framework. We will also consider the fMri dataset in [39], [40].

E. Departures from Existing Works

We now discuss the differences between M-GSP and other existing works.

1) Graph Signal Processing: Generally, M-GSP extends traditional GSP into multilayer networks. We highlight major differences between M-GSP and traditional GSP as follows.

- Geometric model: Traditional GSP [2] applies a single-layer graph, where all nodes are equivalently treated. M-GSP focuses on a more general multilayer model, where different topologies could model different types of connections. In particular, different layers have different physical characteristics and significance, making nodes in different layers unsuited for equivalent treatment in a single supra-graph. On the other hand, different layers are interdependent and cannot be modeled as disjoint individual graphs. Thus, multilayer network is a more general model than normal graphs for graph signal processing.
- Algebraic tools: M-GSP relies on higher degree tensors while GSP relies on second-order tensors. Thus, M-GSP is broadly applicable in high-dimensional data analysis. In particular, if there is only one layer in the multilayer network, the tensor-based analysis simply reduces to matrix-based GSP and is consistent with traditional GSP.
- Flattening: Flattening analysis is an important operation in M-GSP. Flattening the fourth-order tensor into second-order supra-matrix, the M-GSP, with M layers and N nodes in each layer, is equivalent to traditional GSP with MN nodes. However, with flattening analysis, one can only extract the joint information based on the reshaped eigenvectors. To capture the separate information of layer and entity, we still need to apply unflattened M-GSP.

Overall, by extending GSP, M-GSP is both more general and novel, capable of extracting more underlying data features by involving multiple layers of high-dimensional connections.

2) Multi-Way Graph Signal Processing: In [18], MWGSP has been proposed to process high-dimensional signals. Given Kth-order high-dimensional signals, one can decompose the tensor signal in different orders, and construct one graph for each. Graph signal is said to reside on a high-dimensional product graph obtained by the product of all individual factor graphs. Although the MW-GFT is similar to M-GFT for $K = 2$, there still are notable differences in terms of spectrum. First, MWGSP can only process signals without exploiting a given structure since multiple graph spectra would arise from each order of the signals. For a multilayer network with an explicit structure, MWGSP does not naturally process it efficiently and cohesively. Second, MWGSP restricts the types of manageable multilayer network structure. For example, in a spatial temporal dataset, a product graph, formed by the product of spatial connections and temporal connections, has the same topology in each layer. However, many practical systems and datasets showcase more complex geometric interactions. M-GSP provide a more intuitive and natural framework for such multilayer networks. In summary, despite some shared similarities between MW-GFT and M-GFT in some scenarios, they serve different purposes and are suitable for different underlying data structures.

V. Conclusions

In this two-part series, we present a novel tensor-based framework of multilayer network signal processing (M-GSP) that naturally generalizes the traditional GSP to multilayer networks. Part I presents the basic foundation and definitions of M-GSP including MLN signals, signal shifting, spectral space, singular space and MLN frequency. We also provide interpretable discussion and physical insights through numerical results and examples to illustrate the strengths, the general insights, and the benefits that can be obtained from M-GSP. Furthermore, M-GSP exhibits great potentials in practical applications, particularly with respect to more intricate data structures. We shall demonstrate the broad applicability of M-GSP in Part II [21] of this work.

References

[1] A. Sandryhaila, and J. M. F. Moura, "Discrete signal processing on graphs" *IEEE Transactions on Signal Processing*, vol. 61, no. 7, pp. 1644-1656, Apr. 2013.

[2] A. Ortega, P. Frossard, J. Kovačević, J. M. F. Moura and P. Vandergheynst, "Graph signal processing: overview, challenges, and applications," in *Proceedings of the IEEE*, vol. 106, no. 5, pp. 808-828, May 2018.

[3] D. I. Shuman, S. K. Narang, P. Frossard, A. Ortega and P. Vandergheynst, "The emerging field of signal processing on graphs: extending high-dimensional data analysis to networks and other irregular domains," in *IEEE Signal Processing Magazine*, vol. 30, no. 3, pp. 83-98, May 2013.

[4] A. Sandryhaila and J. M. F. Moura, "Discrete signal processing on graphs: frequency analysis," in *IEEE Transactions on Signal Processing*, vol. 62, no. 12, pp. 3042-3054, Jun., 2014.

[5] S. Chen, A. Sandryhaila, J. M. F. Moura and J. Kovacevic, "Signal denoising on graphs via graph filtering," *2014 IEEE Global Conference on Signal and Information Processing (GlobalSIP)*, Atlanta, GA, USA, Dec. 2014, pp. 872-876.

[6] S. Chen, D. Tian, C. Feng, A. Vetro and J. Kovačević, "Fast resampling of three-dimensional point clouds via graphs," in *IEEE Transactions on Signal Processing*, vol. 66, no. 3, pp. 666-681, Feb., 2018.

[7] S. Chen, A. Sandryhaila, J. M. F. Moura and J. Kovačević, "Adaptive graph filtering: multiresolution classification on graphs," *2013 IEEE Global Conference on Signal and Information Processing*, Austin, TX, USA, Dec. 2013, pp. 427-430.

[8] S. Zhang, Z. Ding and S. Cui, "Introducing hypergraph signal processing: theoretical foundation and practical applications," in *IEEE Internet of Things Journal*, vol. 7, no. 1, pp. 639-660, Jan. 2020.

[9] S. Barbarossa and S. Sardellitti, "Topological signal processing over simplicial complexes," in *IEEE Transactions on Signal Processing*, vol. 68, pp. 2992-3007, Mar. 2020.

[10] M. De Domenico, A. Sole-Ribalta, E. Cozzo, M. Kivela, Y. Moreno, M. A. Porter, S. Gomez, and A. Arenas, "Mathematical formulation of multilayer networks," in *Physical Review X*, vol. 3, no. 4, p. 041022, Dec. 2013.

[11] M. Kivelä, A. Arenas, M. Barthelemy, J. P. Gleeson, Y. Moreno, and M. A. Porter, "Multilayer networks," in *Journal of complex networks*, vol. 2, no. 3, pp. 203-271, Jul. 2014.

[12] Boccaletti, G. Bianconi, R. Criado, C. I. Del Genio, J. Gomez- Gardenes, M. Romance, I. Sendina-Nadal, Z. Wang, and M. Zanin, "The structure and dynamics of multilayer networks," *Physics Reports*, vol. 544, no. 1, pp. 1-122, Nov. 2014.

[13] S. Zhang, H. Zhang, H. Li and S. Cui, "Tensor-based spectral analysis of cascading failures over multilayer complex systems," in *Proceedings of 56th Annual Allerton Conference on Communication, Control, and Computing (Allerton)*, Monticello, USA, Oct. 2018, pp. 997-1004.

[14] Z. Huang, C. Wang, M. Stojmenovic, and A. Nayak, "Characterization of cascading failures in interdependent cyberphysical systems," *IEEE Transactions on Computers*, vol. 64, no. 8, pp. 2158-2168, Aug. 2015.

[15] S. V. Buldyrev, R. Parshani, G. Paul, H. E. Stanley, and S. Havlin, "Catastrophic cascade of failures in interdependent networks," *Nature*, vol. 464, no. 7291, pp. 1025-1028, Apr. 2010.

[16] P. Das and A. Ortega, "Graph-based skeleton data compression," *2020 IEEE 22nd International Workshop on Multimedia Signal Processing (MMSP)*, Tampere, Finland, Sep. 2020, pp. 1-6.

[17] F. Grassi, A. Loukas, N. Perraudin and B. Ricaud, "A time-vertex signal processing framework: scalable processing and meaningful representations for time-series on graphs," in *IEEE Transactions on Signal Processing*, vol. 66, no. 3, pp. 817-829, Feb. 2018

[18] J. S. Stanley, E. C. Chi and G. Mishne, "Multiway graph signal processing on tensors: integrative analysis of irregular geometries," in *IEEE Signal Processing Magazine*, vol. 37, no. 6, pp. 160-173, Nov. 2020.

[19] H. Wang, Q. Li, G. D. Agostino, S. Havlin, H. E. Stanley, and P. Van Mieghem, "Effect of the interconnected network structure on the epidemic threshold," *Physical Review E*, vol. 88, no. 2, p. 022801, Aug. 2013.

[20] M. De Domenico, V. Nicosia, A. Arenas, and V. Latora, "Structural reducibility of multilayer networks," *Nature Communications*, vol. 6, no. 6864, pp. 1-9, Apr. 2015.

[21] S. Zhang, Q. Deng and Z. Ding, "Graph signal processing over multilayer networks – part ii: useful tools and practical applications." Supplements.

[22] A. Sandryhaila, and J. M. F. Moura, "Discrete signal processing on graphs: graph Fourier transform," in *Proceedings of 2013 IEEE International Conference on Acoustics, Speech and Signal Processing*, Vancouver, BC, Canada, May 2013, pp. 26-31.

[23] S. Chen, R. Varma, A. Sandryhaila and J. Kovačević, "Discrete Signal Processing on Graphs: Sampling Theory," in *IEEE Transactions on Signal Processing*, vol. 63, no. 24, pp. 6510-6523, Dec.15, 2015.

[24] A. Sandryhaila, and J. M. F. Moura, "Discrete signal processing on graphs: graph filters," in *Proceedings of 2013 IEEE International Conference on Acoustics, Speech and Signal Processing*, Vancouver, Canada, May 2013, pp. 6163-6166.

[25] T. G. Kolda and B. W. Bader, "Tensor decompositions and applications," *SIAM Review*, vol. 51, no. 3, pp. 455-500, Aug. 2009.

[26] H. A. L. Kiers, "Towards a standardized notation and terminology in multiway analysis," *Journal of Chemometrics: A Journal of the Chemometrics Society*, vol. 14, no. 3, pp. 105-122, Jan. 2000.

[27] L. De Lathauwer, B. De Moor, and J. Vandewalle, "A multilinear singular value decomposition," *SIAM Journal on Matrix Analysis and Applications*, vol. 21, no. 4, pp. 1253-1278, Jan. 2000.

[28] A. Afshar, J. C. Ho, B. Dilkina, I. Perros, E. B. Khalil, L. Xiong, and V. Sunderam, "Cp-ortho: an orthogonal tensor factorization framework for spatio-temporal data," in *Proceedings of the 25th ACM SIGSPATIAL International Conference on Advances in Geographic Information Systems*, Redondo Beach, CA, USA, Jan. 2017, p. 67.

[29] I. V. Oseledets, "Tensor-train decomposition," *SIAM Journal on Scientific Computing*, vol. 33, no. 5, pp. 2295-2317, Jun. 2011.

[30] A. C. Kinsley, G. Rossi, M. J. Silk, and K. VanderWaal, "Multilayer and multiplex networks: an introduction to their use in veterinary epidemiology," *Frontiers in Veterinary Science*, vol. 7, p. 596, Sep. 2020.

[31] M. De Domenico, C. Granell, M. A. Porter, and A. Arenas, "The physics of spreading processes in multilayer networks," *Nature Physics*, vol. 12, no. 10, pp. 901-906, Aug. 2016.

[32] E. Valdano, L. Ferreri, C. Poletto, and V. Colizza, "Analytical computation of the epidemic threshold on temporal networks," *Physical Review X*, vol. 5, no. 2, p. 021005, Apr. 2015.

[33] A. Loukas, "Graph reduction with spectral and cut guarantees," *Journal of Machine Learning Research*, vol. 20, no. 116, pp. 1-42, Jun. 2019.

[34] S. Mallat, *A Wavelet Tour of Signal Processing, 3rd ed.* New York, NY, USA: Academic, 2008.

[35] Durrett, Richard, *Random Graph Dynamics*. Cambridge, MA, USA: Cambridge University Press, 2007.

[36] CMU, "Carnegie Mellon University Graphics Lab: Motion Capture Database," accessed on Apr. 21, 2016. [Online]. Available: http://mocap.cs.cmu.edu

[37] N. Vannieuwenhoven, R. Vandebril and K. Meerbergen, "A new truncation strategy for the higher-order singular value decomposition," in *SIAM Journal on Scientific Computing*, vol. 34, no.2 , pp. 1027-1052, Apr. 2012.

[38] L. Durak, and O. Arikan, "Short-time fourier transform: two fundamental properties and an optimal implementation," *IEEE Transactions on Signal Processing*, vol. 51, no. 5, pp. 1231-1242, May 2003.

[39] Z. Wang, Y. Zheng, D. C. Zhu, A. C. Bozoki and T. Li, "Classification of alzheimer's disease, mild cognitive impairment and normal control subjects using resting-state fMRI based network connectivity analysis," in *IEEE Journal of Translational Engineering in Health and Medicine*, vol. 6, pp. 1-9, Oct. 2018.

[40] Y. Liang, Y. Zheng, B. Renli, D. C. Zhu, F. Yu, and T. Li, "Dynamic functional connectivity fading analysis and classification of alzheimer's disease, mild cognitive impairment and normal control subjects based on resting-state fmri data", *OBM Neurobiology* vol. 4, np. 2, Jun. 2020.